Fungal Biology 128 (2024) 2157–2166

Contents lists available at ScienceDirect

Fungal Biology

journal homepage: www.elsevier.com/locate/funbio

Pisolithus microcarpus isolates with contrasting abilities to colonise *Eucalyptus grandis* exhibit significant differences in metabolic signalling

Kanchan Vishwakarma [a,b], Scott Buckley [a], Jonathan M. Plett [c], Judith Lundberg-Felten [d], Sandra Jämtgård [a,b,*], Krista L. Plett [e]

[a] Department of Forest Ecology and Management, Swedish University of Agricultural Sciences, SE-901 83, Umeå, Sweden
[b] Umeå Plant Science Centre, Department of Forest Genetics and Plant Physiology, Swedish University of Agricultural Sciences, Umeå, SE-901 83, Sweden
[c] Hawkesbury Institute for the Environment, Western Sydney University, Richmond, NSW, 2753, Australia
[d] Department of Forest Mycology and Plant Pathology, Uppsala BioCenter, Swedish University of Agricultural Sciences, 750 07, Uppsala, Sweden
[e] NSW Department of Primary Industries and Regional Development, Elizabeth Macarthur Agricultural Institute, Menangle, NSW, 2568, Australia

ARTICLE INFO

Handling Editor: Dr R Balestrini

Keywords:
Ectomycorrhizal fungi
Isolates
Eucalyptus
Metabolites
Indirect contact
Microdialysis system

ABSTRACT

Biotic factors in fungal exudates impact plant-fungal symbioses establishment. Mutualistic ectomycorrhizal fungi play various ecological roles in forest soils by interacting with trees. Despite progress in understanding secreted fungal signals, dynamics of signal production *in situ* before or during direct host root contact remain unclear. We need to better understand how variability in intra-species fungal signaling at these stages impacts symbiosis with host tissues. Using the ECM model *Pisolithus microcarpus*, we selected two isolates (Si9 and Si14) with different abilities to colonize *Eucalyptus grandis* roots. Hypothesizing that distinct early signalling and metabolite profiles between these isolates would influence colonization and symbiosis, we used microdialysis to non-destructively collect secreted metabolites from either the fungus, host, or both, capturing the dynamic interplay of pre-symbiotic signalling over 48 hours. Our findings revealed significant differences in metabolite profiles between Si9 and Si14, grown alone or with a host root. Si9, with lower colonization efficiency than Si14, secreted a more diverse range of compounds, including lipids, oligopeptides, and carboxylic acids. In contrast, Si14's secretions, similar to the host's, included more aminoglycosides. This study emphasizes the importance of intra-specific metabolomic diversity in ectomycorrhizal fungi, suggesting that early metabolite secretion is crucial for establishing successful mutualistic relationships.

1. Introduction

The ecological role of genetically diverse mycobionts that establish on/in tree roots is of great interest for understanding processes associated to plant health and nutrient cycling. Amongst these, ectomycorrhizal (ECM) fungi colonise the roots of most forest trees and can contribute to host nutrition by weathering minerals and mobilizing nutrients from organic material in exchange for plant sugars, making the host and ECM ecologically dependent upon each other (Landeweert et al., 2001; Read and Perez-Moreno, 2003; Nehls et al., 2010; Diagne et al., 2013). ECM fungi include a diverse range of genera and species with distinct phenotypes associated to nutrient acquisition and cycling, stress tolerance, and interaction strategies such as colonization patterns, or mutualistic versus opportunistic behaviour with host plants. Therefore, the ecological impact of these fungi on forest health is strongly linked to ECM fungal diversity in soils. Several recent studies have demonstrated that inter-species ECM diversity and richness within a single host root system enhance tree nutrition (Baxter and Dighton, 2001; Köhler et al., 2018; Khokon et al., 2023). Less often considered, however, is how intra-species diversity on a root system may also contribute to host health. Early studies demonstrate that intra-species variation can significantly impact ECM nitrogen acquisition from organic sources (Anderson et al., 1999; Sawyer et al., 2003; Guidot et al., 2005), nutrient trading (Plett K et al., 2021a; Hortal et al., 2017) and host interactions (Hazard et al., 2017a; Wong et al., 2019). This intra-species variation may also interact with nutrient availability. For example, in *Laccaria bicolor* colonised *Pinus sylvestris* seedlings, fungal intra-species identity significantly impacted the plant biomass but only under inorganic nutrient amendment (Hazard et al., 2017a). When studying *Eucalyptus grandis/Pisolithus microcarpus* interactions, it was

* Corresponding authorDepartment of Forest Ecology and Management, Swedish University of Agricultural Sciences, SE-901 83, Umeå, Sweden.
E-mail address: sandra.jamtgard@slu.se (S. Jämtgård).

https://doi.org/10.1016/j.funbio.2024.09.001
Received 29 March 2024; Received in revised form 1 August 2024; Accepted 5 September 2024
Available online 10 September 2024
1878-6146/© 2024 The Authors. Published by Elsevier Ltd on behalf of British Mycological Society. This is an open access article under the CC BY license (http://creativecommons.org/licenses/by/4.0/).

found that one isolate of *P. microcarpus* had a higher capacity to form ECM roots under reduced glucose concentration as opposed to three other isolates of the same fungal species that reduced host colonisation with reduced glucose (Plett K et al., 2021a). As intra-species identity and richness can contribute to increased plant root productivity and number of ECM-associated roots (Hazard et al., 2017b), it is important to improve our understanding of the pathways controlling host colonisation within ECM fungal species.

The interaction between ECM fungi and the host depends upon initiation and maintenance of complex signalling pathways (Daguerre et al., 2016). The signalling and inter-species fungal competition governing tree root colonisation by diverse ECM individuals is not well understood (Kennedy, 2010; Kennedy et al., 2011, 2020; Queralt et al., 2019). Early host specific signals exuded into the rhizosphere within hours to days during the initiation of the symbiosis might be crucial in how the colonization evolves (Plett and Martin, 2012; Wong et al., 2019; Plett K et al., 2021b). These signals include sugars and other carbon rich compounds (Lagrange et al., 2001; Martin et al., 2001), volatile compounds, metabolites, phytohormones. Fungal effectors such as the mycorrhiza-induced small secreted proteins (MiSSPs) released by ECM fungi are also crucial to establish symbiosis with host roots (Martin et al., 2008; Plett et al., 2011; Plett and Martin, 2012; Doré et al., 2015; Martin et al., 2016). While it is widely established that signals are exchanged between the partners before they come into physical contact, there is still a knowledge gap on how ECM genetic diversity affects this signalling and the impact of released compounds on host trees. In a study by Wong et al. (2019), different isolates of the ECM fungus *P. microcarpus* were tested for metabolite secretion during pre-symbiosis with *Eucalyptus grandis*. The metabolome profiling of fungus-exposed host root tips suggested a significant connection of the root metabolite responses toward the microbial species during pre-symbiotic contact (within 24 h) with later colonization success in *P. microcarpus* isolates. Results are based on destructively harvested tissues and do therefore not capture the secreted metabolites in real time. Methods such as hydroponics (Johansson et al., 2008, 2009; De Vries et al., 2019), solid phase extractions (Menotta et al., 2004) or direct sampling using bulk root tissue (Tschaplinkski et al., 2014; Wong et al., 2019, 2020) have been used to identify metabolites in ECM interactions. However, it is challenging to sample metabolites secreted *in situ* across time since they are either present in low amounts or are modified rapidly (Oburger and Jones, 2018). One way to overcome this is through the use of microdialysis, which offers lower risk of chemical alteration of metabolites during sample processing compared to other methods and allows for continuous sampling. The microdialysis technique, originally developed for neuroscience applications, is a passive diffusion method (Delgado et al., 1972) that allows the sampling of chemical compounds *in vivo* and *in vitro* in plant tissues (Pretti et al., 2014; Plett K et al., 2021b) as well as in soil (Buckley et al., 2020). In a previous study, this technique enabled the continuous, non-destructive sampling of metabolites secreted by fungus and plant during the initiation of the ECM symbiosis between *P. microcarpus* isolate Si14 and *E. grandis* over 48 h. By using this technique, alterations in secreted secondary metabolites were characterised during the early stages of pre-symbiotic signalling (Plett K et al., 2021b).

In the present study, we extended this work to compare early symbiotic signalling between two isolates of *P. microcarpus* with known differences in colonisation potential for their host *E. grandis*: isolate Si9, with low colonization rates, and isolate Si14 with high colonization rates (Plett et al., 2015). Given the previously observed metabolite differences in *E. grandis* roots in pre-symbiotic contact with different isolates of *P. microcarpus* (Wong et al., 2019), we hypothesize that differences in early signalling and metabolite profiles would also be apparent at the interface of the fungus and the root, in addition to metabolite differences within roots in the presence of various fungal isolates. This variability could potentially explain the capacity of the fungal isolates to form symbiotic relationships with their host, *E. grandis*. We also determined if differences in secreted metabolites were also apparent in the free-living mycelium of each isolate and at different time points of early signalling in the presence of a plant.

2. Materials and methods

2.1. Biological material and growth conditions

P. microcarpus isolates Si9 and Si14 (Plett et al., 2015) were sub-cultured on full strength Melin-Norkrans media (MMN) media (0.50 g/l $(NH_4)_2HPO_4$, 0.30 g/l KH_2PO_4, 0.14 g/l of $MgSO_4$*$7H_2O$ and 10 g/l glucose combined with 1 ml/l of 5 % (w/v) $CaCl_2$ stock solution, 1 ml/l of 2.5 % (w/v) NaCl stock solution, 1 ml/l of 0.3 % (w/v) $ZnSO_4$ stock solution, 133 μl/l of 0.1 % (w/v) thiamine stock solution and 1 mL/l of 1.25 % (w/v) citric acid + FeEDTA stock solution, brought to pH 5.5 before the addition of 13 g/l of agar) and grown at room temperature in the dark for one month. Small 1 × 1 cm squares were cut from the growing edges of the fungal colony and placed onto fresh half strength MMN media [1/2 MM N; 0.25 g/l $(NH_4)_2HPO_4$, 0.15 g/l KH_2PO_4, 0.07 g/l of $MgSO_4$.7H2O and 1 g/l glucose combined with 0.5 ml/l of 5 % (w/v) $CaCl_2$ stock solution, 0.5 ml/l of 2.5 % (w/v) NaCl stock solution, 0.5 ml/l of 0.3 % (w/v) $ZnSO_4$ stock solution, 66 μl/l of 0.1 % (w/v) thiamine stock solution and 0.5 ml/l of 1.25 % (w/v) citric acid + FeEDTA stock solution, with pH set to 5.5 before adding 13 g/l of agar] covered with sterilized cellophane membrane (prepared as described in Felten et al., 2009). Plates were then incubated at 28 °C for two weeks.

Eucalyptus grandis seeds (CSIRO tree seed centre, lot 21,068) were sterilized using 30 % H_2O_2 for 10 min and were rinsed three times in sterile water before being plated on 1 % agar media inside a biological safety cabinet. These seeds were then kept inside a walk-in growth chamber (Kryo-Service Oy, Helsinki, Finland) for a duration of four weeks with 12-h day/night cycles, with temperature conditions of 25 °C day/22 °C night, a humidity level of 70 %, and a light intensity of 250 μmol/m^2/s. After this, the seedlings were moved to new 120 mm square Petri plates with 1/2 strength MMN media. To avoid desiccation and prevent the roots from growing into the media (to minimise root breakage during transfer to test plates and minimise adherence of media), sterile cellophane membranes were positioned above and below the roots of each of the three seedlings present on each plate. Following this, the seedlings were kept to grow for another four weeks in the same environmental conditions as described above, within the growth chamber.

2.2. Experimental design

The experiments were set up according to our previous methodology (Plett K et al., 2021b). Briefly, plates were assembled using 120 mm square Petri dishes with half strength MMN, low glucose (0.1 g/l) containing one microdialysis probe (30 mm × 0.5 mm, 20 kDa MWCO, CMA20, CMA Microdialysis AB, Solna, Sweden) per plate to acquire metabolites released by the organism(s) (Fig. S1). To easily pass the microdialysis lead from the plate, holes were created by burning the side corner of the upper lid. The conditions were: six replicates of fungus only (Si9 or Si14), 12 replicates each of plant only, Si9+Plant, Si14+Plant, and duplicate media control.

To establish indirect pre-symbiotic contacts, all components were put together in petri dishes to achieve the different conditions (fungus only, plant + fungus, plant only and media control) according to Plett et al. (2021b). A semi-permeable cellophane membrane was utilized to physically separate plant roots and fungal colonies. This membrane only allows the passage of small proteins and signalling compounds between the two symbionts. The order of placement of membranes and symbionts was: (1) cellophane on the surface of media, (2) 8-week-old *E. grandis* seedling, (3) a microdialysis probe close to the seedling's roots, (4) a cellophane membrane, and (5) a two-week-old fungal colony (Fig. 1A; Plett K et al., 2021b). Plant-only plates had a similar setup but without the fungal colony. Similarly, fungus-only plates had everything except

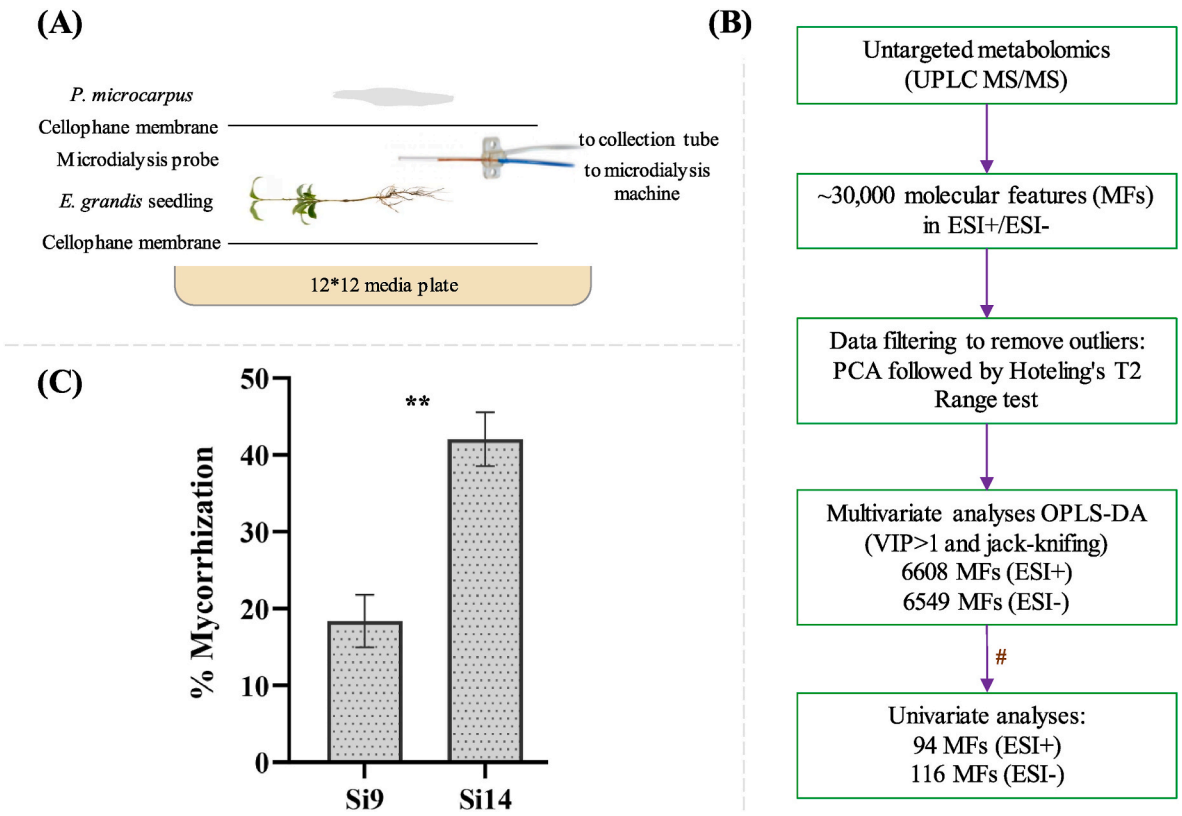

Fig. 1. (A) A schematic representation of a side-view of an *in vitro* plate-based microdialysis system with the probe sampling metabolites during indirect contact between *P. microcarpus* (Si9 and Si14) and *E. grandis* seedlings (modified with permission from Plett et al., 2021b) (B) Percentage of mycorrhizal roots with the two *P. microcarpus* isolates Si9 and Si14 on *E. grandis* roots (n = 5, error bars represent standard error). Mycorrhization percentage was calculated for five replicates per isolate in direct contact with *E. grandis* roots for two weeks ($p < 0.05$ according to unpaired t-test) (C) Flow chart describing major steps in analysing and filtering the metabolomics data obtained from the 48-h time point samples for ESI+ and ESI- modes (# refers to Fig. S2 which includes further steps for filtering the metabolite features).

plants, and media controls were devoid of both fungal colony and plants. The Petri dishes were put together and placed directly in the growth chamber (12-h day/night cycles, 25 °C day/22 °C night) with the probe being connected to infusion pumps (CMA 4004; CMA Microdialysis AB, Solna, Sweden) perfused with sterilized MilliQ water at 5 μl/min flow rate. The dialysate (solution collected by the probe) containing metabolites was collected in a 2 ml screw cap vial at 4 °C. Sampling was done at 0 h, 8 h, 24 h, 32 h and 48 h post plant-fungus contact and 200 μl of each dialysate sample was flash frozen in liquid nitrogen and was then freeze-dried for 48 h (LaboGene CoolSafe Pro 110-4 Allerød, Denmark) and stored at −80 °C.

Additionally, for five replicates per isolate, plates were assembled as above, however, without a microdialysis probe or a cellophane layer separating the fungus from the plant. These plates were maintained in the growth chamber for two weeks to allow for the formation of mature mycorrhizal root tips and assess colonisation rates. Percent mycorrhization was determined by counting the number of mycorrhizal root tips exhibiting the formation of a mantle based on visual assessment under a stereomicroscope and dividing this by the total number of lateral roots in contact with fungal mycelium (x100 %).

2.3. Metabolite analysis

The preparation and metabolite analysis of stored samples was performed according to our previous study (Plett K et al., 2021b). Briefly, 10 μl of cold water, methanol, and formic acid (50/49.9/0.1) were added to the dried samples followed by vortex and sonication for 5 min. Subsequently, the solution was directly injected into a Waters nano-ACQUITY UltraPerformance Liquid Chromatography system (Waters, Wilmslow, UK) that was coupled to a SYNAPT G2-S Mass Spectrometer (Waters, Wilmslow, UK). During the analysis, the samples were run in parallel with a pooled biological quality control sample (obtained by mixing small volumes of various samples across all conditions), method blanks (obtained from microcosms with only media), and true blanks (consisting of only the resuspension solution). The instrument was operated in both positive (ESI+) and negative (ESI-) electrospray ionisation modes. High-resolution mode was used in conjunction with ion mobility to improve the separation of ions.

2.4. Data pre-processing and analysis

Progenesis QI software (Nonlinear Dynamics Ltd., Newcastle upon Tyne, UK) was utilized for the data pre-processing comprising peak picking, peak alignment, and deconvolution. Pre-filtering of the dataset was carried out in SIMCA 17 (Sartorius, Göttingen, Germany) to exclude background, artefacts, and less abundant metabolite features (MFs) by selecting features through principal component analysis (PCA) overview of all samples (Fig. 1B). Filtering or exclusion of MFs and samples was done following two steps (Fig. S2): (i) MFs that were absent in more than 50 % of the samples were removed, and any samples that were missing more than 50 % of MFs were removed from further analyses. Through this, 11,725 MFs from ESI+ and 11,206 MFs from ESI- modes were excluded, and 01 sample from ESI+ and 17 samples from ESI- modes at 48 h were removed from further analyses (Table S1). (ii) Hoteling's T2 range test was conducted on the remaining samples (for four conditions-Si9, Si14, Si9+Plant and Si14+Plant) at all-time points to remove outliers. This test calculates the distance between each sample and the centre of the samples (Hristea, 2004). A value, for a given sample, that

exceeds the critical threshold (95 % T2Crit) indicates that the sample is distant to the rest of the samples in the PCA score-space. Consequently, such samples are likely to be outliers, as their probability of falling in the same group as the other samples is less than 5 %. Through this test, 11 samples from ESI+ and 6 samples from ESI- modes were excluded from further analyses (Table S2, Figs. S3 and S4). The remaining MFs were then transformed by log transformation and UV scaling in SIMCA 17 (Sartorius, Göttingen, Germany). A supervised multivariate analysis, namely orthogonal partial least squares discriminant analysis (OPLS-DA), was used to identify differences between the conditions, i.e. Si9 *vs*. Si14, and Si9+Plant *vs*. Si14+Plant at 48 h time point (Bylesjö et al., 2007). Regression (R^2Y) and cross-validation (Q^2Y) parameters were used to evaluate the OPLS-DA model fitness. The OPLS-DA model is considered as good if $Q^2Y > 0.4$ (Worley and Powers, 2013). MFs highly relevant in differentiating between the conditions in each supervised OPLS-DA model were determined based on variable-in-projection (VIP) scores >1 and jack-knifing (ratio of loadings to confidence interval) for each ionisation mode. Univariate analysis was performed using one-way ANOVA followed by Tukey's post hoc test ($p < 0.05$) using MetaboAnalyst 5.0 (www.metaboanalyst.ca, accessed on 24 April 2023) to evaluate the significance of the MFs that differentiated one condition from the other in the OPLS-DA model and time-based variation of MFs under all conditions. The MFs selected after multivariate (VIP score >1) and univariate analyses (Fig. S2) were used to create the heatmaps using MetaboAnalyst 5.0 through hierarchical clustering of the MFs averaged by a Euclidean distance measure and clustered by the Ward method. Heatmaps plotted the relative levels of each metabolite by mapping numerical values to colors to compare metabolite abundance or intensity across different conditions.

MFs significantly different ($p < 0.05$ through one way ANOVA) in the two comparisons (Si9 *vs*. Si14 and Si9+Plant *vs*. Si14+Plant) were putatively identified using mass and fragmentation scores in Progenesis QI, matching the following databases: HMDB4, MONA, LipidMaps, Metlin, Kegg and CCS (Progenesis library) using a mass error tolerance of 5 ppm, and fragmentation scores >30. Metabolites of synthetic origin or drug or animal-derived were excluded. Also the MFs with 2 M/3 M adducts and scores less than 38 were removed. Adducts (2 M and 3 M) are the products of direct combination of two or more different molecules resulting in one single ion. The scores refer to a metric used to evaluate the match between the observed spectral data of a feature and a reference spectrum for a given compound. Classes were assigned to MFs based on common chemical structures when multiple matches were presented.

3. Results

Secreted metabolite profiles during pre-symbiotic host-fungal interaction differ between P. microcarpus isolates.

The colonisation potential of *E. grandis* by *P. microcarpus* isolate Si14 was significantly higher than by Si9 (Fig. 1C) ($p < 0.05$). In order to understand how the colonization potential is reflected in and explained by the molecular dialogue between the plant and the two fungal isolates, we sampled metabolites by microdialysis. We identified >30,000 secreted MFs in both ESI+ and ESI- modes in samples covering axenically grown plants or fungus as well as early pre-symbiotic plant-fungus contact at time points 0 h, 8 h, 24 h, 32 h and 48 h (Fig. 1B). Considering only the final 48 h time-point, separation of treatment groups was analysed using PCA in which fungus-only groups were clearly separated from all others (Fig. 2A and B). Separation of plant only and pre-symbiosis groups (Si14+Plant and Si9+Plant) were also observed in the ESI- analysis (Fig. 2B).

We used OPLS-DA to identify distinct secreted fungal MFs between the isolates Si9 and Si14 grown axenically, as well as the plant and/or fungal secreted MFs after 48 h of pre-symbiotic interaction for ESI+ and ESI- modes. Based on regression and cross-validation, a clear separation of the metabolite profile of the two fungal isolates (Si9 *vs*. Si14) in both ESI+ and ESI- modes (Fig. 3A and B) and in pre-symbiotic plant-fungus contact (Si14+Plant *vs*. Si9+Plant) for ESI- mode (Fig. 3D) was observed. Although the comparison Si14+Plant *vs*. Si9+Plant in ESI + mode was weakly fitted ($R^2Y = 0.936$, $Q^2Y = 0.236$), several significant MFs ($K_{ESI+} = 1879$) were extracted from this comparison that contributed to the slight separation (Fig. 3C). A total of 4729 (ESI+)/2835 (ESI-) MFs for the fungus-only condition (Si9 *vs*. Si14) and 1879 (ESI+)/3714 (ESI-) MFs in the presence of plants (Si9+Plant *vs*. Si14+Plant) were found to be significantly different (based on VIP score >1 and jack-knifing) (Fig. 1C, Fig. S2, Table S3 and S4). The top 100 MFs based on VIP scores, characterised by high abundance in the respective condition (Si9, Si14, Si9+Plant and Si14+Plant) for each mode were selected. This resulted in a total of 200 MFs in each Si9 *vs*. Si14 and Si9+Plant *vs*. Si14+Plant conditions.

The higher colonising *P. microcarpus* isolate Si14 shows a secreted metabolite profile that is more similar to the host plant alone than the lower colonising isolate Si9.

To further examine the difference in relative abundance of significant MFs across these four conditions (Si9, Si14, Si9+Plant and Si14+Plant), a one-way ANOVA was conducted for the above selected top 200 MFs obtained from each multivariate analysis (OPLS-DA) across all conditions. Based on these results, the 100 most significant MFs among the four conditions (based on ANOVA $p < 0.05$ value) for both Si14 and Si9 were selected and heatmaps showing their relative

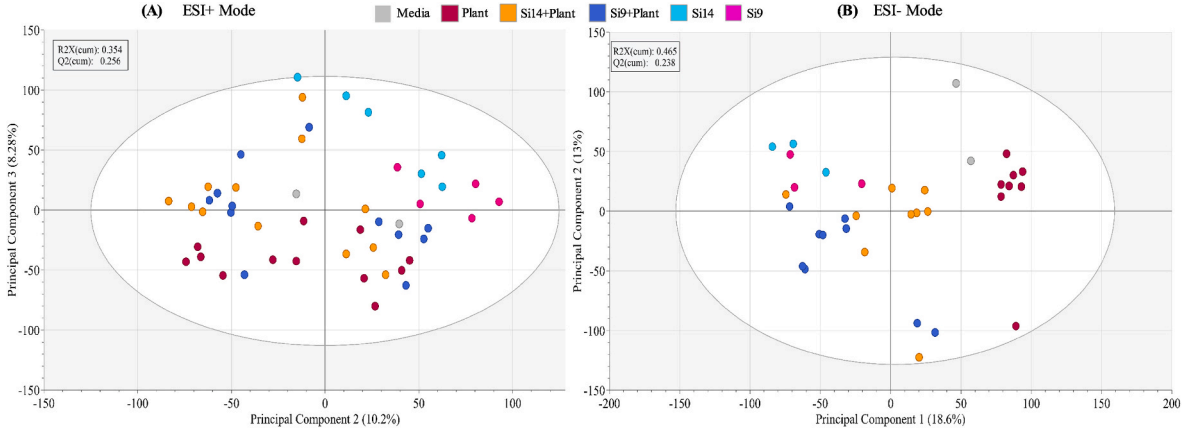

Fig. 2. Principal component analysis (PCA) of all the conditions in (A) ESI + mode and (B) ESI- mode demonstrating the separation of fungus-only groups from the plant groups at 48 h. The outliers excluded are listed in Table S1.

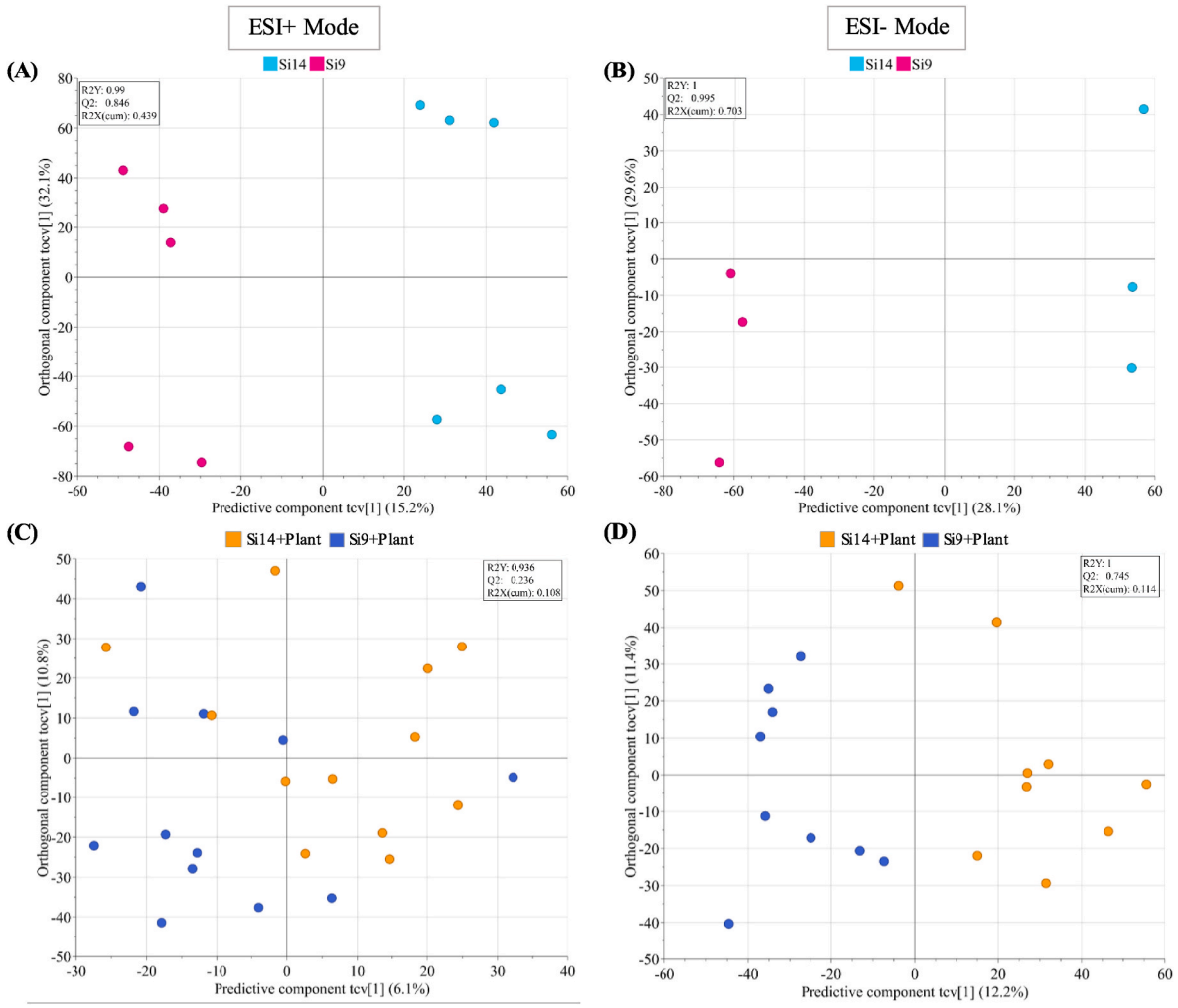

Fig. 3. Supervised multivariate analyses (OPLS-DA) of the fungus-only conditions and indirect contact at 48 h. The comparison between Si9 and Si14 in absence of the host plant in (A) ESI+ and (B) ESI- modes shows clear separation and strong model fitness (Q2Y > 0.4) in the cross-validation (CV) scores plot (C) In ESI + mode, the indirect contact (i.e., Plant + Si9 and Plant + Si14). exhibit overlapping scores, resulting in a weakly fitted model (Q2Y = 0.236) (D) In ESI- mode, the indirect contact show clear separation, with one possible outlier, leading to a well-fitted model (Q2Y = 0.745).

abundance across all conditions were generated (100 MFs total; Fig. 4, Fig. S5). Those MFs with high abundance in the fungal-only groups (when grown axenically) typically showed reduced abundance when the plant was introduced (solid line for Si14 and dashed line for Si9 in Fig. 4A and B). Interestingly, considering the MFs most differentiating the Si9+Plant and Si14+Plant conditions, MFs highly abundant in Si14+Plant conditions were also abundant in plant-only samples (dotted line, Fig. 4C and D), whereas MFs abundant in Si9+Plant conditions were virtually undetectable in plant-only samples (dash-dotted line, Fig. 4C and D).

P. microcarpus isolates Si14 and Si9 demonstrate a differential accumulation of metabolites over time as compared to secreted metabolites in the presence of plant.

For annotation, we considered those MFs from the top 100 lists given in Fig. 4 that showed a significant difference in abundance specifically between the Si9 and Si14 conditions or Si14+Plant and Si9+Plant conditions in both ESI+ and ESI- modes based on ANOVA. This resulted in a total of 94 (42 in Si9 *vs.* Si14 and 52 in Si9+Plant *vs.* Si14+Plant) and 116 MFs (26 in Si9 *vs.* Si14 and 90 in Si9+Plant *vs.* Si14+Plant) in ESI+ and ESI- modes, respectively. These MFs were then searched against different databases for annotation in Progenesis QI software in their respective ionisation modes. Compound classes or putative identifications were assigned to the MFs as available. While most remain unidentified (74 in ESI+ and 103 in ESI-), 20 and 13 MFs in ESI+ and ESI- modes were classified to broad compound classes including amino acids, oligopeptides, terpenoids, fatty acid derivatives, carbohydrates and alkaloids (Table 1).

Using the list of 94 and 116 MFs, we considered their abundance over time (0 h–48 h) within the five different conditions (Plant only, Si9, Si14, Si9+Plant and Si14+Plant) (Fig. 5). Most of the annotated MFs dominant in Si14 (solid line box in Fig. 5) exhibited the highest abundance during the early stages of the interaction (0–8 h) in ESI + mode and contained amino acids and their derivatives. This pattern was also seen in the other fungus containing conditions for these MFs. Few MFs from Si14 showed pronounced abundance towards later stages (32–48 h). For Si9 dominant metabolites (dashed line box in Fig. 5), most of the putatively identified metabolites showed higher abundance towards the 48 h time point and corresponded mostly to peptides and nucleotide sugars. Likewise, the secreted metabolites dominant in the Si9+Plant condition (dash-dotted box in Fig. 5) in both ESI+ and ESI- modes demonstrated a gradual accumulation over time, reaching their peak at the 48 h time point; these included signalling molecules, peptides and lipids classes. A variation in temporal pattern for metabolites dominant in the Si14+Plant condition (dotted box in Fig. 5) was observed in both ESI modes with some occurring abundantly during early interaction and a few increasing in abundance towards 48 h. These mostly involved signalling compounds and carboxylic acid derivatives. From the heatmap (Fig. 5), it was found that many metabolites found highly abundant

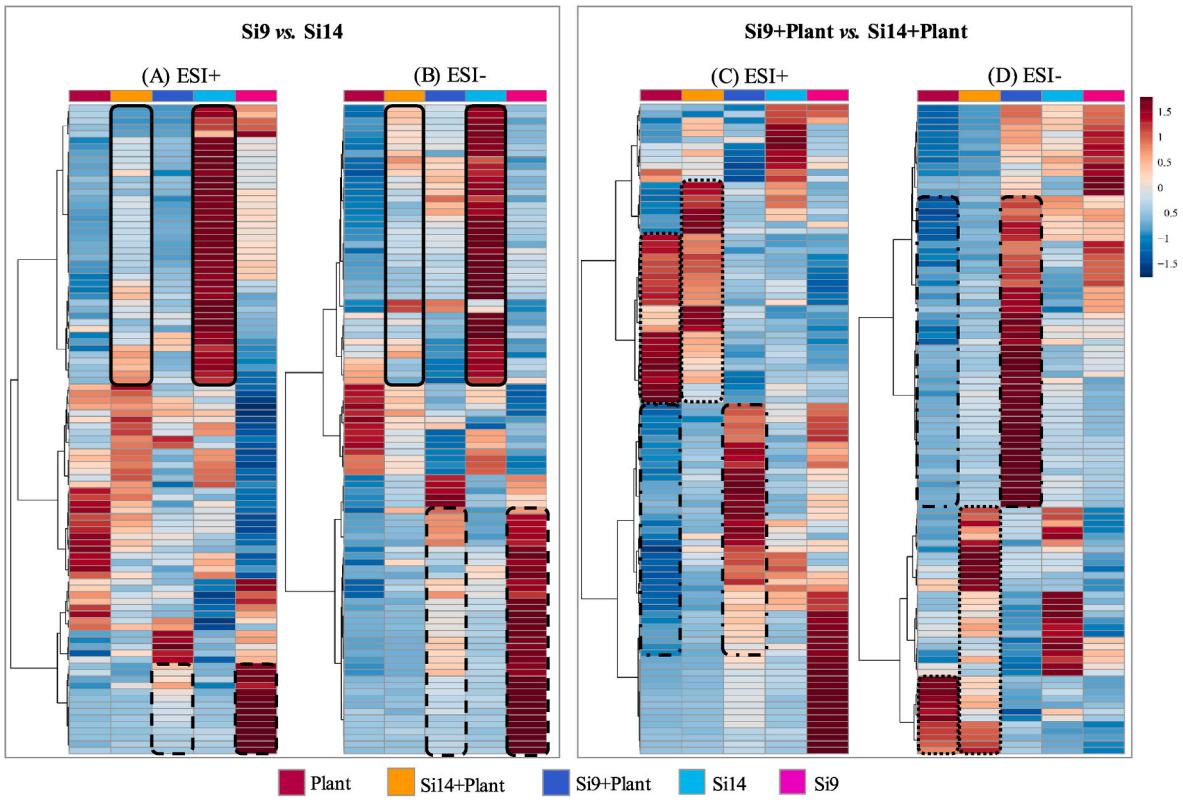

Fig. 4. Heatmaps of the distribution of the top 100 significantly higher and lower abundance of features in both Si9 and Si14 (A, B); and Plant + Si9 and Plant + Si14 (C, D) across all treatment groups at 48 h (listed in bold in Table S2 and Table S3) (A, C represent ESI + mode, and B, D ESI- mode). The significance of features was determined through one-way ANOVA with $p < 0.05$ (Fig. S2). The observations excluded from PCA listed in Table S1 were also excluded from these heatmaps. The data represented is the mean of replicates (n) (ESI + mode: n = 12 for Plant-only, Si9+Plant and Si14+Plant, n = 6 for Si14 and n = 5 for Si9; ESI- mode: n = 8 for Plant-only, n = 9 for Si9+Plant and Si14+Plant, n = 3 for Si14 and Si9). The colour scale represents the distribution and abundance of metabolite peak intensities where blue signifies lower and red signifies higher abundance of metabolites within the dataset. The values −1.5 to 1.5 are based on z-score data scaling which means metabolite levels are 1.5 standard deviations below and above the mean value. The rectangular boxes represent the comparison of metabolite abundance (solid line for Si14 and dashed line for Si9 to compare with their plant counterparts in A and B; and dotted line for Si14+Plant and dash-dotted line for Si9+Plant to compare with plant-only condition in C and D). (For interpretation of the references to colour in this figure legend, the reader is referred to the Web version of this article.)

in Si9+Plant were absent or lowly abundant in plant-only samples. However, interestingly, the metabolite pattern of the Si14+Plant condition at early time points closely resembled the abundance pattern of MFs in the Plant-only condition as also observed in Fig. 4.

4. Discussion

The pre-symbiotic signalling stage of mutualistic establishment between ECM fungi and their hosts serves as a crucial phase during which both organisms undergo noteworthy alterations in physiological and molecular parameters before establishing physical contact. These alterations are induced and facilitated through the exchange and perception of a wide array of metabolic signals. While prior investigations provide evidence that changes in plant metabolites exhibit a degree of selectivity in response to diverse microbial species (Kamilova et al., 2006; Giovannetti et al., 2015; Kelly et al., 2018), our present study sought to extend the understanding on secreted metabolites and their altered abundance during pre-symbiotic signalling between two isolates of the same ectomycorrhizal fungal species (*P. microcarpus*) and *E. grandis* roots.

Our analyses revealed a distinctly different secreted metabolite profiles from axenically grown isolates Si9 and Si14, despite belonging to the same species. These distinctive metabolomic profiles may contribute to the difference in root colonisation observed between these isolates. Si9's profile was enriched in lipids, oligopeptides, and carboxylic acids. These compounds could be involved in maintaining cell structure and facilitating energy metabolism, important in fungal adaptation to environmental stressors (Keyhani 2018; Fedoseeva et al., 2021). Conversely, Si14 produced more aminoglycosides. In support of intra-species variability, studies on *Cenococcum geophilum* (Li et al., 2022) and *Suillus bovinus* (Fransson et al., 2007) demonstrate that metabolic differences between isolates of the same ectomycorrhizal species may be common. The functional implications of these difference must, therefore, be considered when studying the role of ECM fungi in natural settings.

The interaction of the fungal isolates with the plant profoundly influenced the profile of secreted metabolites recovered. While identifying the precise origin of metabolites during indirect contact remains challenging and many could have been of plant origin, we observed a significant shift in metabolites during pre-symbiotic plant-fungus interaction compared to those produced by the fungus or the plant alone. This is consistent with the results of our previous study in which the presence of plant host with *P. microcarpus* significantly altered the metabolites produced in the extra-cellular space (Plett K et al., 2021b). While relatively few metabolomic studies focus on secreted metabolites, other studies in plant–mycorrhizal interactions have observed similar dramatic shifts in metabolite profiles extracted from roots upon the introduction of mycorrhizal fungi (Sebastiana et al., 2021; Wong et al., 2020; Zou et al., 2023; Ghirardo et al., 2020). Interestingly, our results show that the pre-symbiotic interaction between the low root colonizer Si9 and *E. grandis* led to a variety of metabolites that were either not present or only weakly present in the pre-symbiotic interaction between the higher root colonizer Si14 and *E. grandis*. In contrast, the overlap between the MFs of Si14+Plant and Plant-only conditions suggest that

Table 1
Putative compound classes and identifications of metabolic features under conditions in which they are abundant.

Neutral mass (m/z)	Retention time (min)	Conditions	Putative Compound Class	Class colour as per Fig. 5	Putative identity
ESI+ Mode					
534.2846	6.48	Si9	Lipids		
571.3074	6.81	Si14	Aminoglycosides		
215.0664	1.25	Si14	N acyl amino acids		
190.1186	1.77	Si14	Amino acids		
459.2079	5.89	Si14	Oligopeptide		
218.1413	1.27	Si14	Xanthine alkaloids		
416.2689	0.55	Si9+Plant	Triazinanes		N-Eicosapentaenoyl Asparagine
194.1005	0.53	Si9+Plant	Amidines		
441.2239	2.23	Si9+Plant	Sterol esters		
293.1893	2.76	Si9+Plant	Steroids		
322.0574	2.13	Si9+Plant	Dipeptide		gamma-Glu-Met(1-)
418.1578	0.70	Si9+Plant	Oligopeptide		Glu-Thr-Phe
418.1585	0.55	Si9+Plant	Oligopeptide		Glu-Thr-Phe
412.0447	3.60	Si14+Plant	Triazinanes		
371.1356	3.42	Si14+Plant	Phenylpyridines		
494.3329	4.33	Si14+Plant	Fatty acyl amides		
429.1727	4.05	Si14+Plant	Dicarboxylic acid monoamide		Cathestatin B
426.1483	3.74	Si14+Plant	Carboxamide		N-(3-methoxyphenyl)-1-(3-oxo-4H-1,4-benzothiazine-2-carbonyl)piperidine-4-carboxamide
349.0359	3.60	Si14+Plant	Hydroxycoumarin		{[4-(7-methoxy-2-oxo-2H-chromen-6-yl)but-3-en-2-yl]oxy}sulfonic acid
258.1713	2.99	Si14+Plant	Fatty acyls		Hydroxyhexanoycarnitine
ESI- Mode					
306.0986	3.21	Si9	Oligopeptide		glutathione amide
416.0974	3.92	Si9	Carboxylic acids and derivatives		2-O-sinapoyl-D-glucaric acid
453.0617	4.80	Si9	Oligopeptide/ peptide anion		2,4-dinitrophenyl-S-glutathione
673.0548	3.64	Si9	nucleotide sugar oxoanion		UDP-N-acetyl-3-O-(1-carboxylatovinyl)-D-glucosamine(3-)
511.0516	2.92	Si9	nucleotide sugar		dTDP-3-dehydro-4,6-dideoxy-D-glucose
188.9910	1.20	Si9	Fatty Acyls		4-dimethylarsenobutanoic acid
664.1028	3.60	Si14	Sugar alcohol		mannose-(1D-myo-inositol 1-phosphate)2
674.0631	3.54	Si9+Plant	nucleotide sugar oxoanion		UDP-N-acetyl-3-O-(1-carboxylatovinyl)-D-glucosamine(3-)
470.3031	4.07	Si9+Plant	Terpenoid		
371.0233	3.32	Si9+Plant	Dinucleotides		Nicotinate adenine dinucleotide phosphate
408.1417	3.35	Si14+Plant	Sesquiterpenoids		
383.2088	4.21	Si14+Plant	Indoloquinolines		
343.0491	3.55	Si14+Plant	Oligopeptides		glutathione amide

these MFs might be predominantly plant-derived rather than fungal.

Fungal and plant signalling and metabolomic regulation have profound impacts on mycorrhizal interactions, including colonization potential, carbon-nitrogen trading dynamics and nutrient acquisition. Recent studies have demonstrated that mycorrhizal fungi exhibiting high colonisation potential on a host are able to effectively suppress plant immune responses, typically through the activity of effector proteins that act as negative regulators of plant defence genes (Plett et al., 2011; Daguerre et al., 2020; Favre-Godal et al., 2020; Plett et al., 2020; He et al., 2020). Our results would suggest that, in addition to microbial effectors, distinct metabolic patterns between *P. microcarpus* isolates may contribute to their differing mycorrhization potential. Our time course analysis of significant MFs found that metabolites primarily associated with Si14 showed higher abundance at the initial time points (0–8 h), while those primarily associated with fungus Si9 became more dominant as the time progressed to 48 h. It could be hypothesized that metabolite suppression at early time points in Si14 may contribute to root colonization by avoiding host immune system activation. Alternatively, the metabolites seen in the Si9+Plant condition could be primarily of plant origin and indicative of a heightened plant immune response that does not occur in interaction with Si14. Further tests on a broader array of isolates and species should be considered in future to determine if some isolates may adopt a stealth covert strategy, secreting fewer metabolites to avoid triggering the host's immune response.

Recent studies have also shed light on the mechanisms by which mycorrhizal fungi with high colonization potential suppress plant immune responses. Mycorrhizal fungi contain beta-glucan and chitin in their cell walls that are absent from plant walls and can initially trigger plant immune responses during interaction (Bartnicki-Garcia, 1987; Zeng et al., 2020). However, as the symbiotic relationship progresses, these fungi employ strategies to downregulate these immune responses, facilitating successful colonization. For instance, mycorrhizal fungi produce effector proteins that act as negative regulators of plant defence genes, suppressing the production of defence chemicals like salicylic acid, jasmonic acid, and ethylene (Enebe et al., 2023). A notable example is the secretion of MiSSP7 by *L. bicolor*, which interacts with jasmonic acid inducible gene repressors, leading to the downregulation of defence gene expression (Plett et al., 2011; Daguerre et al., 2020; Favre-Godal et al., 2020; He et al., 2020). Similarly, arbuscular mycorrhizal fungi, like *Rhizophagus irregularis*, produce RiSLM (a lysin motif effector), which binds to chitin oligosaccharides on the fungal cell walls, thus protecting them from plant-produced chitinases and subverting chitin-triggered immune responses (Bozsoki et al., 2017; Zeng et al., 2020). These findings highlight the sophisticated biochemical tactics employed by mycorrhizal fungi to modulate plant immune systems, ensuring effective symbiosis formation and nutrient exchange.

Although the exact identification of the metabolites within our samples was impeded due to a lack of known standards, our analyses revealed their classification into prominent metabolite classes, including amino acids, peptides, terpenoids, flavonoids, alkaloids, nucleotide derivatives and fatty acids. Notably, terpenoids and flavonoids have established roles as secreted and volatilised compounds that play pivotal

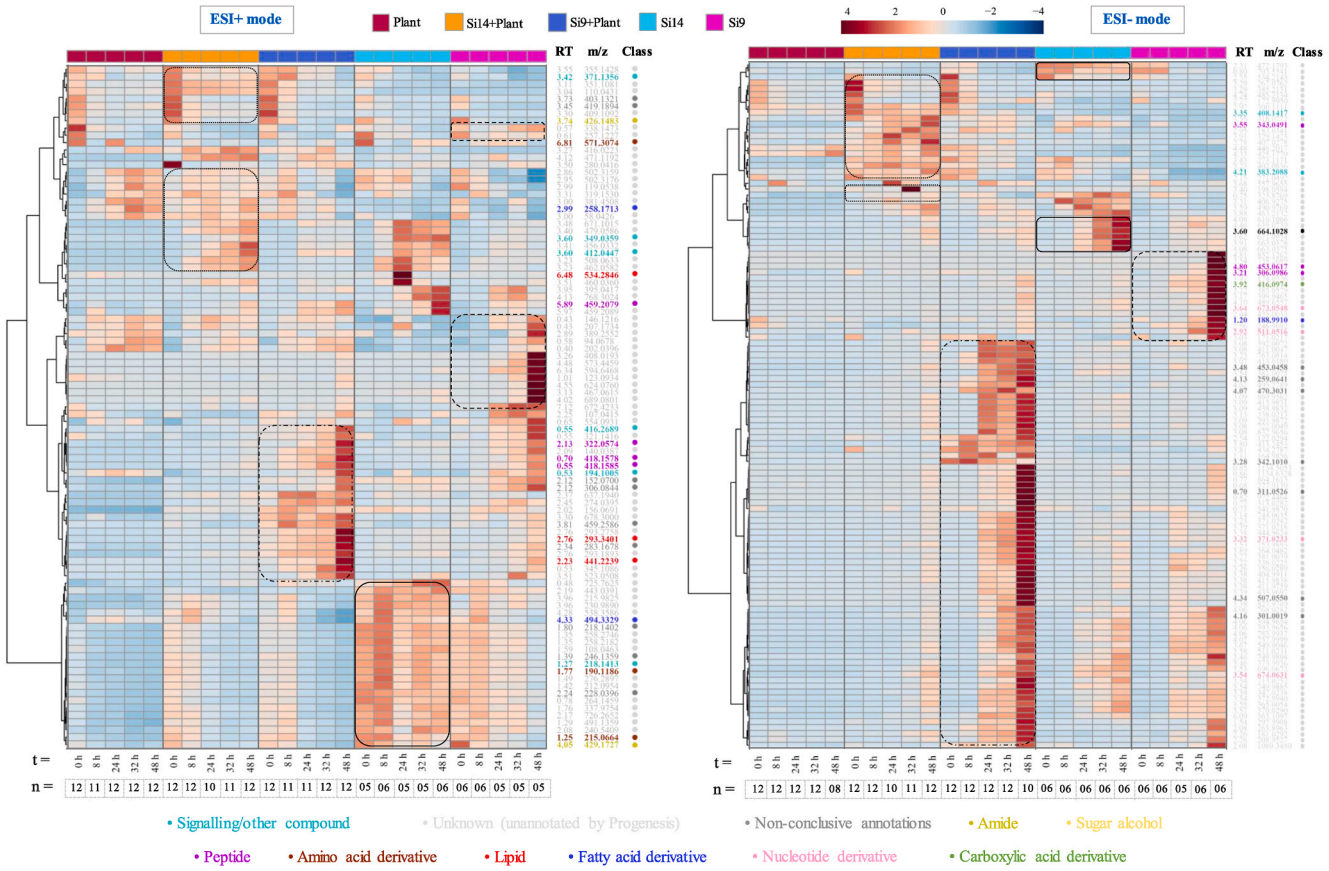

Fig. 5. The time-point distribution of putatively identified significant metabolic features from 0 h to 48 h under different conditions in ESI + mode and ESI- mode. The outliers excluded are listed in Table S2. The data represented is the mean of replicates (n) (t = different time points; n = number of replicates in each time point; RT = retention time; *m/z* = mass to charge ratio; different colour dots represent the putative class of compounds, also specified in Table 1). The solid line represents metabolites for Si14, dashed line for Si9, dotted line for Si14+Plant and dash-dotted line for Si9+Plant metabolites. The colour scale represents the distribution and abundance of values within the data where blue signifies lower and red signifies higher abundance of metabolites within the dataset. The values −4 to 4 are based on z-score data scaling which means metabolite levels are 4 standard deviations below and above the mean value, respectively. (For interpretation of the references to colour in this figure legend, the reader is referred to the Web version of this article.)

roles in mediating microbial interactions (Steinkellner et al., 2007; Plett et al., 2024). Additionally, the widespread involvement of alkaloids is evident as they present dual roles in plant defence mechanisms and growth process regulations (Waller and Nowacki, 1978; Velič;kovic' et al., 2019). The presence of these metabolite classes aligns with studies demonstrating that plant secondary metabolites, including terpenes, quinolone derivatives, phytohormones, and sterols, modulate ectomycorrhizal colonization (Dahm and Golińska, 2011; Marqués-Gálvez et al., 2024). In our dataset, lipids and oligopeptides were among the highly abundant MFs present during pre-symbiotic signalling with host roots with both isolates. In the *P. sylvestris* - *Pisolithus tinctorius* interaction, contrasting lipid compositions between the intraradical and extraradical mycelia of the ECM has been observed (Laczko et al., 2004). This disparity highlights the potential significance of plant lipid translocation, potentially influencing the functionality of ectomycorrhizal symbiosis as lipids may play a role in signalling, energy storage or as structural components of the fungi that could influence fungi's ability to perform symbiotic functions. However, overlapping of certain MFs between fungal only and indirect contact conditions poses challenges in interpreting the effects of these metabolites on the interaction dynamics. Such overlapping metabolites could either play roles in the interaction or represent generalist metabolites (Rey et al., 2013; Miyata et al., 2014; Zhang et al., 2015).

The variability in metabolite abundance at different time points also highlights the intricate and evolving nature of metabolic signalling during the pre-symbiotic phase of these interactions. Over time, lipids, oligopeptides, and nucleotide sugars emerged as predominant compounds released during the later stages of pre-symbiotic interaction, specifically between 32 and 48 h. In contrast, sesquiterpenoids, indoloquinolines, phenylpyridine, hydroxycoumarin, and triazinanes detected in Si14+Plant conditions exhibited distinct temporal abundance patterns with the majority starting to appear from 0 h and decreasing gradually. These metabolites have well-established roles in ectomycorrhizal colonization (Dahm and Golińska, 2011) and in root architecture modification during colonization (Ditengou et al., 2015; Plett et al., 2024) however our findings suggest the timing of their involvement at different stages of symbiotic contact may be important. Notably, these signalling metabolites were absent in the Si9+Plant condition. Wong et al.'s (2019) investigation putatively characterized fatty acid derivatives, alkaloids, and terpenoids after 24 h of pre-symbiotic interaction. Our study also identified these metabolites in both the fungus-only and indirect contact groups, albeit with distinct temporal patterns.

Ectomycorrhizal diversity, both between and within species, is important to optimised tree health and resilience. Understanding the metabolic pathways that impact fungal–host interactions may shed light on how these communities establish. In conclusion, the diversity in metabolite production and colonization strategies among different isolates of the same fungal species, such as *Pisolithus*, may play a crucial role in the dynamics of plant–microbe interactions in forest ecosystems.

CRediT authorship contribution statement

Kanchan Vishwakarma: Writing – original draft, Visualization, Software, Formal analysis, Data curation. **Scott Buckley:** Writing – review & editing, Validation, Investigation, Data curation. **Jonathan M. Plett:** Writing – review & editing, Methodology, Conceptualization. **Judith Lundberg-Felten:** Writing – review & editing, Supervision, Funding acquisition, Conceptualization. **Sandra Jämtgård:** Writing – review & editing, Supervision, Funding acquisition, Resources, Conceptualization. **Krista L. Plett:** Writing – review & editing, Supervision, Funding acquisition, Resources, Methodology, Conceptualization.

Declaration of competing interest

The authors declare that they have no known competing financial interests or personal relationships that could have appeared to influence the work reported in this paper.

Acknowledgements

Authors would like to thank the Western Sydney University Mass Spectrometry Facility and Meena Mikhael for processing metabolomic samples. We also thank Kate Bennett and David Nilsson at The Computational Analytical Support Platform (CASP), Umeå University for support in multivariate data analyses. We acknowledge the statistical advice provided by Hans Stenlund at the Swedish Metabolomics Centre, Umeå University. We also like to thank the financial and resource support from The Swedish Foundation for International Cooperation in Research and Higher Education (STINT) [grant number IB2019-8147], the Kempe Foundations [grant number JCK-2015], and Bio4Energy in facilitating our research.

Appendix A. Supplementary data

Supplementary data to this article can be found online at https://doi.org/10.1016/j.funbio.2024.09.001.

References

Anderson, I.C., Chambers, S.M., Cairney, J.W.G., 1999. Intra- and interspecific variation in patterns of organic and inorganic nitrogen utilization by three Australian *Pisolithus* species. Mycol. Res. 103, 2.

Bartnicki-Garcia, S, 1987. The cell wall: a crucial structure in fungal evolution. Evol. Biol. Fungi. 10, 389–403.

Baxter, J.W., Dighton, J., 2001. Ectomycorrhizal diversity alters growth and nutrient acquisition of grey birch (*Betula populifolia*) seedlings in host–symbiont culture conditions. New Phytol. 152 (1), 139–149.

Bozsoki, Z., Cheng, J., Feng, F., Gysel, K., Vinther, M., Andersen, K.R., et al., 2017. Receptor-mediated chitin perception in legume roots is functionally separable from Nod factor perception. Proc. Nat. Acad. Sci. 114, E8118–E8127.

Buckley, S., Brackin, R., Jämtgård, S., Näsholm, T., Schmidt, S., 2020. Microdialysis in soil environments: current practice and future perspectives. Soil Biol. Biochem. 143, 107743.

Bylesjö, M., Rantalainen, M., Cloarec, O., Nicholson, J.K., Holmes, E., Trygg, J., 2007. OPLS discriminant analysis: combining the strengths of PLD-DA and SIMCA classification. J. Chemometr. 20, 341–351.

Daguerre, Y., Basso, V., Hartmann-Wittulski, S., Schellenberger, R., Meyer, L., Bailly, J., Kohler, A., Plett, J.M., Martin, F., Veneault-Fourrey, C., 2020. The mutualism effector MiSSP7 of *Laccaria bicolor* alters the interactions between the poplar JAZ6 protein and its associated proteins. Sci. Rep. 10 (1), 20362.

Daguerre, Y., Plett, J.M., Veneault-Fourrey, C., 2016. Signaling pathways driving the development of ectomycorrhizal symbiosis. In: Martin, F. (Ed.), Molecular Mycorrhizal Symbiosis. John Wiley & Sons, Ltd, Hoboken, NJ, pp. 141–157.

Dahm, H., Golińska, P., 2011. Ectomycorrhiza and secondary metabolites. In: Rai, M., Varma, A. (Eds.), Diversity and Biotechnology of Ectomycorrhizae. Springer, Berlin Heidelberg, pp. 371–385.

De Vries, F.T., Williams, A., Stringer, F., Willcocks, R., McEwing, R., Langridge, H., Straathof, A.L., 2019. Changes in root-exudate induced respiration reveal a novel mechanism through which drought affects ecosystem carbon cycling. New Phytol. 224, 132–145.

Delgado, J.M., DeFeudis, F.V., Roth, R.H., Ryugo, D.K., Mitruka, B.M., 1972. Dialytrode for long term intracerebral perfusion in awake monkeys. Arch. Int. Pharmacodyn. Ther. 198, 9–21.

Diagne, N., Thioulouse, J., Sanguin, H., Prin, Y., Krasova-Wade, T., Sylla, S., Galiana, A., Baudoin, E., Neyra, M., Svistoonoff, S., Lebrun, M., 2013. Ectomycorrhizal diversity enhances growth and nitrogen fixation of *Acacia mangium* seedlings. Soil Biol. Biochem. 57, 468–476.

Ditengou, F.A., Müller, A., Rosenkranz, M., Felten, J., Lasok, H., Van Doorn, M.M., Legué, V., Palme, K., Schnitzler, J.P., Polle, A., 2015. Volatile signalling by sesquiterpenes from ectomycorrhizal fungi reprogrammes root architecture. Nat. Commun. 6 (1), 6279.

Doré, J., Perraud, M., Dieryckx, C., Kohler, A., Morin, E., Henrissat, B., Lindquist, E., Zimmermann, S.D., Girard, V., Kuo, A., Grigoriev, I.V., 2015. Comparative genomics, proteomics and transcriptomics give new insight into the exoproteome of the basidiomycete *Hebeloma cylindrosporum* and its involvement in ectomycorrhizal symbiosis. New Phytol. 208, 1169–1187.

Enebe, M.C., Erasmus, M., 2023. Susceptibility and plant immune control—A case of mycorrhizal strategy for plant colonization, symbiosis, and plant immune suppression. Front. Microbiol. 14, 1178258.

Favre-Godal, Q., Gourguillon, L., Lordel-Madeleine, S., Gindro, K., Choisy, P., 2020. Orchids and their mycorrhizal fungi: an insufficiently explored relationship. Mycorrhiza 30, 5–22.

Fedoseeva, E.V., Danilova, O.A., Ianutsevich, E.A., et al., 2021. Micromycete lipids and stress. Microbiology 90, 37–55.

Felten, J., Kohler, A., Morin, E., Bhalerao, R.P., Palme, K., Martin, F., Ditengou, F.A., Legué, V., 2009. The ectomycorrhizal fungus *Laccaria bicolor* stimulates lateral root formation in poplar and Arabidopsis through auxin transport and signaling. Plant Physiol. 151 (4), 1991–2005. https://doi.org/10.1104/pp.109.147231.

Fransson, P.M., Anderson, I.C., Alexander, I.J., 2007. Ectomycorrhizal fungi in culture respond differently to increased carbon availability. FEMS (Fed. Eur. Microbiol. Soc.) Microbiol. Ecol. 61 (2), 246–257.

Ghirardo, A., Fochi, V., Lange, B., Witting, M., Schnitzler, J.P., Perotto, S., Balestrini, R., 2020. Metabolomic adjustments in the orchid mycorrhizal fungus *Tulasnella calospora* during symbiosis with *Serapias vomeracea*. New Phytol. 228 (6), 1939–1952.

Giovannetti, M., Mari, A., Novero, M., Bonfante, P., 2015. Early *Lotus japonicus* root transcriptomic responses to symbiotic and pathogenic fungal exudates. Front. Plant Sci. 6, 480.

Guidot, A., Verner, M.C., Debaud, J.C., Marmeisse, R., 2005. Intraspecific variation in use of different organic nitrogen sources by the ectomycorrhizal fungus *Hebeloma cylindrosporum*. Mycorrhiza 15, 3.

Hazard, C., Kruitbos, L., Davidson, H., Mbow, F.T., Taylor, A.F.S., Johnson, D., 2017a. Strain identity of the ectomycorrhizal fungus *Laccaria bicolor* is more important than richness in regulating plant and fungal performance under nutrient rich conditions. Front. Microbiol. 8, 1874.

Hazard, C., Kruitbos, L., Davidson, H., Taylor, A.F., Johnson, D., 2017b. Contrasting effects of intra-and interspecific identity and richness of ectomycorrhizal fungi on host plants, nutrient retention and multifunctionality. New Phytol. 213 (2), 852–863.

He, Q., McLellan, H., Boevink, P.C., Birch, P.R., 2020. All roads lead to susceptibility: the many modes of action of fungal and oomycete intracellular effectors. Plant Communications 1, 100050.

Hortal, S., Plett, K.L., Plett, J.M., Cresswell, T., Johansen, M., Pendall, E., et al., 2017. Role of plant-fungal nutrient trading and host control in determining the competitive success of ectomycorrhizal fungi. ISME J. 11, 12.

Hristea, F., 2004. Outlier detection, Hristea algorithm. In: Encyclopedia of Statistical Sciences.

Johansson, E.M., Fransson, P.M.A., Finlay, R.D., van Hees, P.A.W., 2008. Quantitative analysis of root and ectomycorrhizal exudates as a response to Pb, Cd and as stress. Plant Soil 313, 39–54.

Johansson, E.M., Fransson, P.M.A., Finlay, R.D., van Hees, P.A.W., 2009. Quantitative analysis of soluble exudates produced by ectomycorrhizal roots as a response to ambient and elevated CO2. Soil Biol. Biochem. 41, 1111–1116.

Kamilova, F., Kravchenko, L.V., Shaposhnikov, A.I., Makarova, N., Lugtenberg, B., 2006. Effects of the tomato pathogen *Fusarium oxysporum* f. sp. radicis-lycopersici and of the biocontrol bacterium *Pseudomonas fluorescens* WCS365 on the composition of organic acids and sugars in tomato root exudate. Mol. Plant Microbe Interact. 19, 1121–1126.

Kelly, S., Mun, T., Stougaard, J., Ben, C., Andersen, S.U., 2018. Distinct *Lotus japonicus* transcriptomic responses to a spectrum of bacteria ranging from symbiotic to pathogenic. Front. Plant Sci. 9, 1218.

Kennedy, P., 2010. Ectomycorrhizal fungi and interspecific competition: species interactions, community structure, coexistence mechanisms, and future research directions. New Phytol. 187 (4), 895–910.

Kennedy, P.G., Gagne, J., Perez-Pazos, E., Lofgren, L.A., Nguyen, N.H., 2020. Does fungal competitive ability explain host specificity or rarity in ectomycorrhizal symbioses? PLoS One 15 (8), e0234099.

Kennedy, P.G., Higgins, L.M., Rogers, R.H., Weber, M.G., 2011. Colonization-competition tradeoffs as a mechanism driving successional dynamics in ectomycorrhizal fungal communities. PLoS One 6 (9), e25126.

Keyhani, N.O., 2018. Lipid biology in fungal stress and virulence: entomopathogenic fungi. Fungal Biol. 122 (6), 420–429.

Khokon, A.M., Janz, D., Polle, A., 2023. Ectomycorrhizal diversity, taxon-specific traits and root N uptake in temperate beech forests. New Phytol. 239 (2), 739–751.

Köhler, J., Yang, N., Pena, R., Raghavan, V., Polle, A., Meier, I.C., 2018. Ectomycorrhizal fungal diversity increases phosphorus uptake efficiency of European beech. New Phytol. 220 (4), 1200–1210.

Laczko, E., Boller, T., Wiemken, V., 2004. Lipids in roots of *Pinus sylvestris* seedlings and in mycelia of *Pisolithus tinctorius* during ectomycorrhiza formation: changes in fatty acid and sterol composition. Plant Cell Environ. 27, 27–40.
Lagrange, H., Jay-Allemand, C., Lapeyrie, F., 2001. Rutin, the phenolglycoside from *Eucalyptus* root exudates, stimulates *Pisolithus* hyphal growth at picomolar concentrations. New Phytol. 150, 349–355.
Landeweert, R., Hoffland, E., Finlay, R.D., Van Kuyper, T.W., 2001. Linking plants to rocks: ectomycorrhizal fungi mobilize nutrients from minerals. Trends Ecol. Evol. 16, 248–254.
Li, J., Li, C., Tsuruta, M., et al., 2022. Physiological and transcriptional responses of the ectomycorrhizal fungus *Cenococcum geophilum* to salt stress. Mycorrhiza 32, 327–340.
Marqués-Gálvez, J.E., Pandharikar, G., Basso, V., Kohler, A., Lackus, N.D., Barry, K., Keymanesh, K., Johnson, J., Singan, V., Grigoriev, I.V., Vilgalys, R., 2024. *Populus* MYC2 orchestrates root transcriptional reprogramming of defence pathway to impair *Laccaria bicolor* ectomycorrhizal development. New Phytol. 242, 658–674.
Martin, F., Aerts, A., Ahrén, D., Brun, A., Danchin, E.G., Duchaussoy, F., Gibon, J., Kohler, A., Lindquist, E., Pereda, V., Salamov, A., 2008. The genome of *Laccaria bicolor* provides insights into mycorrhizal symbiosis. Nature 452 (7183), 88–92.
Martin, F., Duplessis, S., Ditengou, F., Lagrange, H., Voiblet, C., Lapeyrie, F., 2001. Developmental cross talking in the ectomycorrhizal symbiosis: signals and communication genes. New Phytol. 151 (1), 145–154.
Martin, F., Kohler, A., Murat, C., Veneault-Fourrey, C., Hibbett, D.S., 2016. Unearthing the roots of ectomycorrhizal symbioses. Nat. Rev. Microbiol. 14 (12), 760–773.
Menotta, M., Gioacchini, A.M., Amicucci, A., Buffalini, M., Sisti, D., Stocchi, V., 2004. Headspace solid-phase microextraction with gas chromatography and mass spectrometry in the investigation of volatile organic compounds in an ectomycorrhizae synthesis system. Rapid Commun. Mass Spectrom. 18, 206–210.
Miyata, K., Kozaki, T., Kouzai, Y., Ozawa, K., Ishii, K., Asamizu, E., et al., 2014. The bifunctional plant receptor, OsCERK1, regulates both chitin-triggered immunity and arbuscular mycorrhizal symbiosis in rice. Plant Cell Physiol. 55, 1864–1872.
Nehls, U., Göhringer, F., Wittulsky, S., Dietz, S., 2010. Fungal carbohydrate support in the ectomycorrhizal symbiosis: a review. Plant Biol. 12 (2), 292–301.
Oburger, E., Jones, D.L., 2018. Sampling root exudates—mission impossible? Rhizosphere 6, 116–133.
Plett, J.M., Kemppainen, M., Kale, S.D., Kohler, A., Legué, V., Brun, A., Tyler, B.M., Pardo, A.G., Martin, F., 2011. A secreted effector protein of *Laccaria bicolor* is required for symbiosis development. Curr. Biol. 21 (14), 1197–1203.
Plett, J.M., Kohler, A., Khachane, A., Keniry, K., Plett, K.L., Martin, F., Anderson, I.C., 2015. The effect of elevated carbon dioxide on the interaction between *Eucalyptus grandis* and diverse isolates of *Pisolithus* sp. is associated with a complex shift in the root transcriptome. New Phytol. 206, 1423–1436.
Plett, J.M., Martin, F., 2012. Poplar root exudates contain compounds that induce the expression of MiSSP7 in *Laccaria bicolor*. Plant Signal. Behav. 7 (1), 12–15.
Plett, J.M., Wojtalewicz, D., Plett, K.L., Collin, S., Kohler, A., Jacob, C., Martin, 2024. Sesquiterpenes of the ectomycorrhizal fungus *Pisolithus microcarpus* alter root growth and promote host colonization. Mycorrhiza 34, 69–84. Epub ahead of print. PMID: 38441669.
Plett, K.L., Buckley, S., Plett, J.M., Anderson, I.C., Lundberg-Felten, J., Jämtgård, S., 2021b. Novel microdialysis technique reveals a dramatic shift in metabolite secretion during the early stages of the interaction between the ectomycorrhizal fungus *Pisolithus microcarpus* and its host *Eucalyptus grandis*. Microorganisms 9 (9), 1817.
Plett, K.L., Kohler, A., Lebel, T., Singan, V.R., Bauer, D., He, G., Ng, V., Grigoriev, I.V., Martin, F., Plett, J.M., Anderson, I.C., 2021a. Intra-species genetic variability drives carbon metabolism and symbiotic host interactions in the ectomycorrhizal fungus *Pisolithus microcarpus*. Environ. Microbiol. 23 (4), 2004–2020.
Plett, J.M., Plett, K.L, Wong-Bajracharya, J., de Freitas Pereira, M., Costa, M.D., Kohler, A., Martin, F., Anderson, I.C., 2020. Mycorrhizal effector PaMiSSP10b alters polyamine biosynthesis in Eucalyptus root cells and promotes root colonization. New Phytol 228, 712–727.
Pretti, L., Bazzu, G., Serra, P.A., Nieddu, G., 2014. A novel method for the determination of ascorbic acid and antioxidant capacity in *Opuntia ficus indica* using in vivo microdialysis. Food Chem. 147, 131–137.
Queralt, M., Walker, J.K., De Miguel, A.M., Parladé, J., Anderson, I.C., Hortal, S., 2019. The ability of a host plant to associate with different symbiotic partners affects ectomycorrhizal functioning. FEMS (Fed. Eur. Microbiol. Soc.) Microbiol. Ecol. 95 (6), fiz069.
Read, D.J., Perez-Moreno, J., 2003. Mycorrhizas and nutrient cycling in ecosystems – a journey towards relevance? New Phytol. 157, 475–492.
Rey, T., Nars, A., Bonhomme, M., Bottin, A., Huguet, S., Balzergue, S., et al., 2013. NFP, a LysM protein controlling Nod factor perception, also intervenes in *Medicago truncatula* resistance to pathogens. New Phytol. 198, 875–886.
Sawyer, N.A., Chambers, S.M., Cairney, J.W.G., 2003. Variation in nitrogen source utilisation by nine *Amanita muscaria* genotypes from Australian *Pinus radiata* plantations. Mycorrhiza 13, 4.
Sebastiana, M., Gargallo-Garriga, A., Sardans, J., Pérez-Trujillo, M., Monteiro, F., Figueiredo, A., Maia, M., Nascimento, R., Silva, M.S., Ferreira, A.N., Cordeiro, C., 2021. Metabolomics and transcriptomics to decipher molecular mechanisms underlying ectomycorrhizal root colonization of an oak tree. Sci. Rep. 11 (1), 8576.
Steinkellner, S., Lendzemo, V., Langer, I., Schweiger, P., Khaosaad, T., Toussaint, J.-P., et al., 2007. Flavonoids and strigolactones in root exudates as signals in symbiotic and pathogenic plant-fungus interactions. Molecules 12, 1290–1306.
Tschaplinkski, T.J., Plett, J.M., Engle, N.L., Deveau, A., Cushman, K.C., Martin, M.Z., Doktycz, M.J., Tuskan, G.A., Brun, A., Kohler, A., et al., 2014. *Populus trichocarpa* and *Populus deltoides* exhibit different metabolomic responses to colonization by the symbiotic fungus *Laccaria bicolor*. Mol. Plant Microbe Interact. 27, 546–556.
Veličković, D., Liao, H.L., Vilgalys, R., Chu, R.K., Anderton, C.R., 2019. Spatiotemporal transformation in the alkaloid profile of *Pinus* roots in response to mycorrhization. J. Nat. Prod. 82 (5), 1382–1386.
Waller, G.R., Nowacki, E.K., 1978. Alkaloid Biology and Metabolism in Plants. Springer, Boston, MA.
Wong, J.W., Lutz, A., Natera, S., Wang, M., Ng, V., Grigoriev, I., Martin, F., Roessner, U., Anderson, I.C., Plett, J.M., 2019. The influence of contrasting microbial lifestyles on the pre-symbiotic metabolite responses of *Eucalyptus grandis* roots. Frontiers in Ecology and Evolution 7, 10.
Wong, J.W.H., Plett, K.L., Natera, S.H.A., Roessner, U., Anderson, I.C., Plett, J.M., 2020. Comparative metabolomics implicates threitol as a fungal signal supporting colonization of *Armillaria luteobubalina* on eucalypt roots. Plant Cell Environ. 43, 374–386.
Worley, B., Powers, R., 2013. Multivariate analysis in metabolomics. Current Metabolomics 1, 92–107.
Zeng, T., Rodriguez-Moreno, L., Mansurkhodzaev, A., Wang, P., van den Berg, W., Gasciolli, V., et al., 2020. A lysin motif effector subverts chitin-triggered immunity to facilitate arbuscular mycorrhizal symbiosis. New Phytol 225, 448–460.
Zhang, X., Dong, W., Sun, J., Feng, F., Deng, Y., He, Z., et al., 2015. The receptor kinase CERK1 has dual functions in symbiosis and immunity signalling. Plant J. 81, 258–267.
Zou, Y.N., Qin, Q.Y., Ma, W.Y., Zhou, L.J., Wu, Q.S., Xu, Y.J., Kuča, K., Hashem, A., Al-Arjani, A.B., Almutairi, K.F., Abd-Allah, E.F., 2023. Metabolomics reveals arbuscular mycorrhizal fungi-mediated tolerance of walnut to soil drought. BMC Plant Biol. 23 (1), 1–4.